

## Laser Damage to Metallic Targets of Different Thermal Properties

**T. El Dessouki, I. Fouda\*, F. Sharaf\*\* and N. Khalil**

*College of Science, King Abdul Aziz University, Jeddah, Saudi Arabia*

**ABSTRACT.** An empirical formula is applied to relate the laser-induced damage to single metallic films to their thermal properties. The dependence of the resulting damage into targets of double metallic layers on their thicknesses is investigated. The damage into the double layer target is found to be four times greater than its value for the corresponding thickness in the single layer case, when the laser powder pulse is kept constant.

Laser technology attains progressively more and more interest due to the ever increased applications. The advent of the laser has produced a light source of high enough power that considerable heating effects may be generated when the light is absorbed. These phenomena have aroused considerable interest (Chik 1974, Von Allmen 1976). The most spectacular effects, involving a change of phase of the absorbing material, have been investigated by Ready (1965).

Barakat *et al.* (1980) studied the resultant damage on glass and stainless steel targets due to the thermal effect of laser beams. They determined interferometrically the depth of the resultant crater. The dependence of the evaporated material, as well as the depth of the depression and the depressed area, on the applied tube voltage of the laser pulse have been determined. Comparison of the rates of propagation was also carried out.

The thermal effect of lasers on glass substrates coated by different thin metal films of silver, copper, aluminium, nickel, chromium and antimony was studied by

\* Faculty of Science, Mansoura Univ., Mansoura, Egypt.

\*\* Atomic Energy Establishment, Cairo, Egypt.

El-Dessouki *et al.* (1984). They showed that the depression in the damaged area is linearly dependent on the thickness of the metal films as well as on their thermal conductivities. The depressions are found to be greater than those produced in uncoated glass.

The scanning electron microscope was employed by Sharaf *et al.* (1979) for direct observation of the morphological changes produced from the pits and their surroundings when thin metallic films of silver, copper and aluminium deposited on glass substrates are irradiated by pulsed ruby laser. Different shapes, grain boundaries, molten zones and crystalline forms were closely studied. The observations were indicative of the mode of deformation which is attributed to thermal effects.

In the present work, an empirical formula is investigated, for the first time, relating the maximum depression of the resulting damage into glass substrates coated by single layers of various thickness of silver, copper, aluminium, nickel, chromium and antimony to their thermal properties. The target is subjected to the focused Q-switched ruby laser pulse ( $\lambda = 649.3$  nm) of intensity  $10 \text{ MW/cm}^2$  with duration time of 30 n sec. The laser radiation is focused onto the surface of the target within an area of  $250 \mu\text{m}$  in diameter by using an objective lens  $\times 16/0.2$ .

Furthermore, the resulting damage into glass substrates coated by double layers of some of these metals is also studied.

Meanwhile, the morphological features of the different phases of the damaged regions in the irradiated targets are studied further by the scanning electron microscope.

### Investigated Empirical Formula

The depression of the resultant damage into substrates coated by single metals has been studied before by El-Dessouki *et al.* (1984) and is represented by Fig. 1a. A new empirical formula is investigated in the present work, relating the resultant damage to the thermal properties of the target. Consequently, each of the six curves of Fig. 1a can be illustrated as in Fig. 1b, in which its slope can be given by:

$$\frac{D - A}{T - b} = m \quad (1)$$

where,  $D$  is the depression of the resultant damage in ( $\mu\text{m}$ );  $T$  is the metal film thickness in ( $\mu\text{m}$ );  $a$  is the value of depression at the common intersection points, in ( $\mu\text{m}$ );  $b$  is the value of the thickness at the intersection point of the curves in ( $\mu\text{m}$ ); and  $m$  is the slope of each curve.

Examining the slopes of the curves, it is found that the slope  $m$  for each curve is directly proportional to the thermal conductivity  $K$  of the specific metal, and

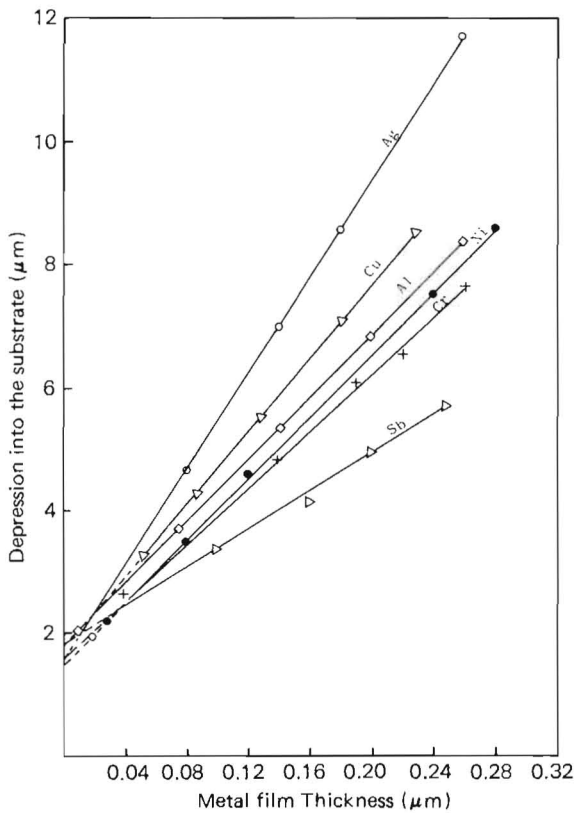


**Fig. 1a.** The relation between the maximum depression into the glass substrate and the metallic film thickness.

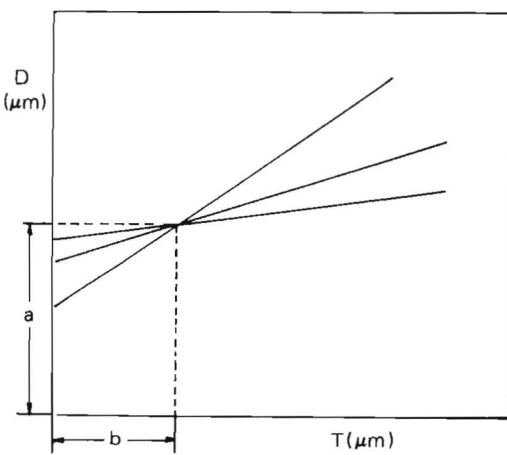


**Fig. 1b.** Symbolic representation of Fig. 1a.

inversely proportional to the square root of its melting point  $M$  and its boiling point  $B$ . Thus, Eq. (1) reduces to

$$\frac{D - a}{T - b} = C \cdot \frac{K}{\sqrt{BM}} \quad (2)$$

where  $C$  is a constant of units  $\text{Cal}^{-1} \text{Cm degree}^{-2} \text{sec.}$

Equation (2) is found applicable, yielding a constant  $C$  of the same value for each of the two groups having high and low conductivities. The resultant values of the constant  $C$  for the different six metals of the target are shown in Table 1. By substituting the values of  $K$ ,  $M$  and  $B$  from tables (Robert 1976), the constant  $C$  is found to have value  $(7.2 \pm 0.4) \times 10^4$  for high conductivities films of silver, copper and aluminium. Meanwhile,  $C$  is found to have the value  $(29.2 \pm 2.8) \times 10^4$  for films having low conductivities; namely, nickel, chromium and antimony.

When considering the thermal conductivities of the metals at higher temperatures the constant  $C$  of Eq. (2) does not change appreciably, while the order is kept constant.

A good agreement between the experimental results using the empirical formula is quite clear for both groups as the constant  $C$  has a value of the same order. The difference between the values of that constant could be related to the effect of other physical parameters such as the reflectivity of the metallic film, specific heat and thermal expansion. Reflectivity plays an effective role in the power of the incident laser beam through the target. Such factors will be investigated later.

### Damage into Targets with Double Layer Metallic Films

The results of damage of single metallic layers on glass substrates showed that the resultant damage depends on the thermal properties of the target. Further

**Table 1.** The resultant constant  $C$  of the six different metals of the target, considering their physical constants at room temperature.

Metal symbol	Melting point (M) $^\circ\text{K}$	Boiling Point B( $^\circ\text{K}$ )	Thermal conductivity K( $\text{Watt cm}^{-1} \text{K}^{-1}$ )	C ( $\text{Cal}^{-1} \text{cm S. K}^{-2}$ )
Ag	1235	2485	4.29	$7.2 \times 10^4$
Cu	1356	2840	4.01	$6.3 \times 10^4$
Al	933	2740	2.37	$7.2 \times 10^4$
Ni	1726	3005	0.909	$26.8 \times 10^4$
Cr	2130	2945	0.939	$26.3 \times 10^4$
Sb	904	2023	0.244	$32.4 \times 10^4$

evidence could be obtained by investigating the resultant damage of double metallic films of different thermal properties.

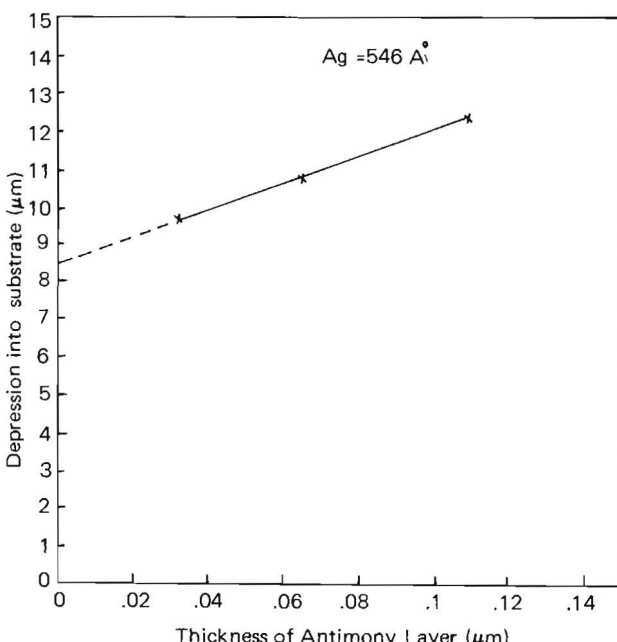
For this purpose, targets consisting of two groups are prepared. In the first group, glass substrates coated by a thermally conductive metallic film (silver), over which layers of different thicknesses of metallic films of lower thermal properties (antimony), are deposited. The thickness of the silver film was 546 Å, while the thickness of antimony layer ranged between 327 and 1192 Å. In the second group, the glass substrates are coated by a layer of antimony of thickness 682 Å, over which silver layers, of different thicknesses ranging between 320 and 1760 Å, are deposited. The techniques of shooting and measurements adopted for the case of double layer targets are the same as those applied in the single layer targets (El Dessouki *et al.* 1984).

Figure 2 represents the obtained results for the first group. It shows the dependence of the resultant damage into the substrate on the thickness of the antimony layer facing the laser beam while a silver layer of thickness 546 Å is deposited between antimony and the glass substrate. A linear relation is also found as in the case of single layer films. However, the value of the resultant damage into the double layer target is found to be four times greater than its value for the corresponding thickness in the single layer case, when the laser power is kept constant.

This may be attributed to the combined effects of the antimony layer of low melting point and the silver layer of high thermal conductivity. The antimony layer melts locally by the laser beam absorbing most of its thermal energy. This considerable energy is transferred to the silver layer concentrating it into the substrate. Deeper damage is thus produced. Such an explanation can be supported by the obtained slopes of silver and antimony in Fig. 1a.

The extrapolation of the curve in Fig. 2 shows that the depression into the substrate of double layer with 548 Å silver and zero thickness of antimony is 8.5  $\mu\text{m}$ ; whereas, from Fig. 1, the depression into the substrate coated by 546 Å single silver layer is 3.8  $\mu\text{m}$ . By comparing the two values of depression for a silver layer of 546 Å thickness, it is found that the extrapolated value of depression into the substrate of double layer is twice that in case of single layer. This may be ascribed to the presence of antimony in double layer. Due to the low melting and boiling points of antimony, the thermal energy of laser beam is easily absorbed by antimony film and then transferring it to the silver layer.

Unfortunately, the resultant damage in the second group, where the silver layer is facing the laser beam, while the antimony layer of low melting point lies between glass and silver, could not be related to the metallic film thickness. This may be attributed to the diffusion of the silver into the antimony layer forming a new metallurgical phase that calls for further studies.



**Fig. 2.** The relation between the resultant damage into the substrate and the thickness of the antimony layer coated over a silver layer of thickness 546 Å.

### Morphological Features of the Damaged Targets

By focusing the light of a high power pulsed laser on a target surface, one is able to evaporate selectively material from a minute and well localized surface area of the target under study. After stopping the stimuli, evaporated atoms from the laser-heated zone are brought onto the surface and recrystallized forms appear. Consequently, the thermal properties of the irradiated metal film play main roles, not only on the depth of the resulting depression, as shown above, but also on the resulting morphological features as revealed by the electron microscope. It is the objective of this section to show how far both effects are related together and to the material thermal properties.

Plates 1-4 show the morphological features of the damaged areas. The evaporated material flows away from the center of irradiation due to the thermal gradient, leaving behind it a resultant pit. After stopping the stimuli, the molten material will begin to recrystallize at the colder regions in the surroundings of the pit. The crystallization is controlled by factors such as the thermal gradient, the interphase forces, the rate of flow and growth, that are directly dependent on the thermal properties of the target.

Plate (1) illustrates the general features of an irradiated target with an antimony film: a pit (A) surrounded by two regions (B) and (C) that had been rearranged due to the formation of high temperature centers throughout the specimen during irradiation. The two regions of material seem in primary stages of phase transformation as a result of the temperature gradient. So, plastic deformation can be observed associated with displacement of the atoms from their original positions within the grains, causing permanent changes in the shape of the target and its surroundings. Different forms of crystals are observed (rhombic and rhombohedral forms).

Plate 2 shows a part of the same region in plate 1 with higher magnification and in another tilted position. More distinct grain boundaries, voids, loops and gas bubbles due to the adsorption of gases, are observed. Further, as the silicon substrate is heated to a high temperature, amorphous silicon behaves in the same manner as crystalline silicon. It partially melts and becomes crystalline by cooling. Plate 2, thus, shows observably different shapes of loops, of which the silicon dioxide ( $\text{SiO}_2$ ) loops appear.

On the other hand, Plate 3 shows an electronmicrograph of a pit and its surroundings in an irradiated glass substrate coated by a nickel film of thickness 0.08  $\mu\text{m}$ . Melted zones, intercrystalline cracks, voids, different shapes of crystals and gas bubbles can be observed. The pit A is surrounded by a material B which has melted and resolidified again. The molten zone extended beyond the pit. Clearly, it could not migrate indefinitely, due to a regime of great complexity. This regime is controlled by factors such as the ability of the melt to spread over the substrate surface. This phenomenon is controlled by the relative values of interfacial and surface energy between the substrate and the melt. The important parameters affecting the migration of the melt are the thermal properties of the target as well as the substrate temperature and introduction of gaseous impurities.

Different shapes of crystals are shown. These are due to condensation from the vapour state on the surface at atmospheric pressure; some interaction with atmospheric oxygen and nitrogen caused the forms of crystals shown in Plate 3.

Plate 4 is an SEM micrograph showing evidence that high temperature centers and high pressure centers are produced in the form of gas bubbles, the expansion of which leads to wedging of the coated material and formation of cracks. Plate 4 shows a dark cavity A made up of cracks beside regions B and C, showing a reformation of lamellae from nickel. Region C appears as aggregate lamellae (like a flower), caused by radial high pressure and temperature, during the course of crack expansion.



**Plate 1.** SEM micrograph of the pit in a damaged glass substrate coated by an antimony film.

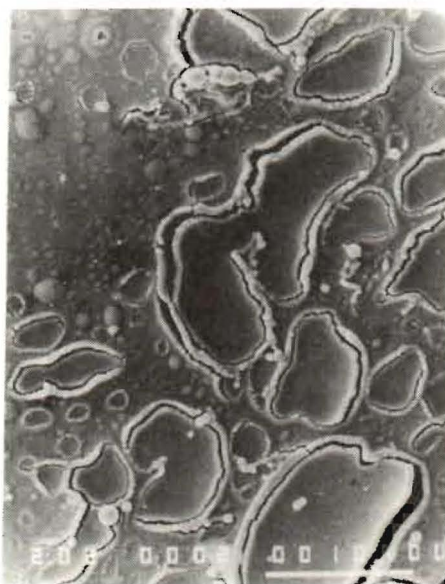


**Plate 2.** SEM micrograph inside the damaged area of glass substrate coated by an antimony film.



**Plate 3.** SEM micrograph showing the pit and its surroundings in a glass substrate coated by a nickel film.

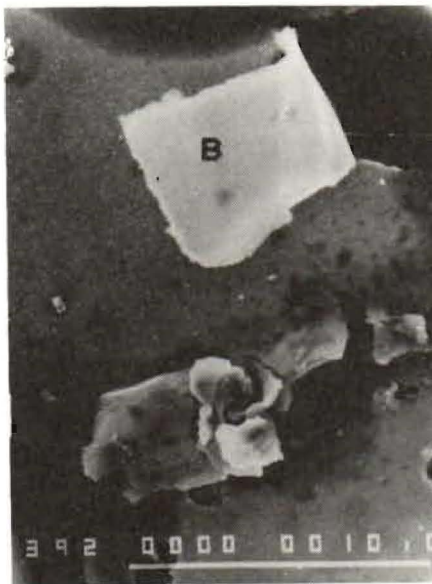


**Plate 4.** SEM micrograph outside the pit in a glass substrate coated by a nickel film.

### References

- Barakat, N., El-Dessouki, T. and Sharaf, F.** (1980) Laser induced damage to glass and stainless steel target, *J. Optics (Paris)* **11**: 123-126.
- Chik, K.P.** (1974) Laser damage in glass due to a metal film, *Thin Solid Films ((Switzerland))* **21**: 527-530.
- El-Dessouki, T., Sharaf, F., Fouda, I. and Khalil, N.** (1984) Laser damage measurements in glass substrates coated by metallic films, *Arab Gulf J. scient. Res.* **2**: 199-207.
- Ready, J.F.** (1965) Effects due to absorption of laser radiation, *J. appl. Phys.* **36**: 462-468.
- Robert, C.W. ed.** (1975-1976) *Hand-Book of Chemistry and Physics*, 56th edition, CRC press, Cleveland, Ohio, B-1, E-12.
- Sharaf, F., Fouda, I. and El-Dessouki, T.** (1979) Scanning electron microscopical investigation of thin metallic films irradiated by laser, *Mansoura Sci. Bull.* **7**: 199-208.
- Von Allmen, M.** (1976) Laser drilling velocity in metals, *J. appl. Phys.* **47**: 5460-5463.

(Received 29/02/1984;  
in revised form 03/10/1984)

## إتلاف الليزر داخل أهداف معدنية ذات خواص حرارية مختلفة

توفيق الدسوقي، إبراهيم فودة<sup>\*</sup>، فؤاد شرف<sup>\*\*</sup> و نجوى خليل

كلية العلوم - جامعة الملك عبد العزيز - جدة - المملكة العربية السعودية

تم تطبيق صيغة تجريبية جديدة على العلاقة التي تربط بين الإتلاف التأثيرى لشعاع الليزر داخل أغشية معدنية رقيقة وخواصها الحرارية. كما درست العلاقة التجريبية بين الإتلاف الناتج داخل أهداف مغطاة بغشاء معدنى مزدوج وسمك الغشاء. ووُجد أن الإتلاف داخل الأهداف المغطاة بشرائح معدنية مزدوجة أكبر أربع مرات من قيمة الإتلاف الناتج من نفس شعاع الليزر عندما يسقط على أهداف مغطاة بغشاء معدنى منفرد له نفس السمك.

<sup>\*</sup> كلية العلوم - جامعة المنصورة - المنصورة - مصر

<sup>\*\*</sup> مؤسسة الطاقة الذرية - القاهرة - مصر